

Transition between strong and weak topological insulator in ZrTe_5 and HfTe_5

Zongjian Fan¹, Qi-Feng Liang², Y. B. Chen³, Shu-Hua Yao¹, and Jian Zhou^{1,4,*}

¹National Laboratory of Solid State Microstructures and Department of Materials Science and Engineering, Nanjing University, Nanjing 210093, China

²Department of Physics, Shaoxing University, Shaoxing 312000, China

³National Laboratory of Solid State Microstructures and Department of Physics, Nanjing University, Nanjing 210093, China

⁴Collaborative Innovation Center of Advanced Microstructures, Nanjing University, Nanjing, 210093, China.

*Corresponding author: zhoujian@nju.edu.cn

ABSTRACT

ZrTe_5 and HfTe_5 have attracted increasingly attention recently since the theoretical prediction of being topological insulators (TIs). However, subsequent works show many contradictions about their topological nature. Three possible phases, i.e. strong TI, weak TI, and Dirac semi-metal, have been observed in different experiments until now. Essentially whether ZrTe_5 or HfTe_5 has a band gap or not is still a question. Here, we present detailed first-principles calculations on the electronic and topological properties of ZrTe_5 and HfTe_5 on variant volumes and clearly demonstrate the topological phase transition from a strong TI, going through an intermediate Dirac semi-metal state, then to a weak TI when the crystal expands. Our work might give a unified explain about the divergent experimental results and propose the crucial clue to further experiments to elucidate the topological nature of these materials.

Introduction

Topological insulator (TI) is a new class of material which is an insulator in its bulk, while having time reversal symmetry protected conducting states on the edge or surface.¹⁻³ A large number of realistic materials have been theoretically proposed and experimentally confirmed, such as Bi_2Se_3 and Bi_2Te_3 .^{4,5} However, the layered transition-metal pentatelluride ZrTe_5 and HfTe_5 is a particular example. ZrTe_5 and HfTe_5 were studied more than 30 years ago due to the large thermoelectric power⁶ and mysterious resistivity anomaly.^{7,8} Recently, Weng *et al.* predicted that mono-layer ZrTe_5 and HfTe_5 are good quantum spin Hall insulators with relatively large bulk band gap (about 0.1 eV) by first principles calculations.⁹ The three-dimensional (3D) bulk phase of ZrTe_5 and HfTe_5 are also predicted to be TIs, which are located at the vicinity of a transition between strong and weak TI, but without detailed description.⁹

Nevertheless, subsequent experiments show many contradictions about the topological nature of ZrTe_5 or HfTe_5 . Several experimental works suggested that ZrTe_5 is a Dirac semi-metal without a finite band gap by different characterization methods, such as Shubnikov-de Haas oscillations, angle-resolved photoemission spectroscopy (ARPES), and infrared reflectivity measurements.¹⁰⁻¹⁵ Of course there are also other experimental works holding opposite point of view. For example, in two recent scanning tunneling microscopy (STM) experiments, they unambiguously observed a large bulk band gap about 80 or 100 meV in ZrTe_5 ,^{16,17} implying that there is no surface state on the top surface and therefore ZrTe_5 should be a weak TI. Another APRES work also favored a weak TI for ZrTe_5 .¹⁸ However, there are two other ARPES works which believed that ZrTe_5 is a strong TI.^{19,20} For instance, by using the comprehensive ARPES, STM, and first principles calculations, Manzoni *et al.* found a metallic density of state

(DOS) at Fermi energy, which arises from the two-dimensional surface state and thus indicates ZrTe_5 is a strong TI.¹⁹

The divergence of these experiments make ZrTe_5 (HfTe_5) being a very puzzling but interesting material, which needs more further experimental and theoretical studies. Therefore, in order to figure out the physical mechanism behind those contradictory experimental results, we revisited the band structures of ZrTe_5 and HfTe_5 , and carefully studied their relationship with the volume expansion. We find a clear topological transition between a strong and weak TI in ZrTe_5 and HfTe_5 , accompanied by an intermediate Dirac semi-metal state between them. This work could shed more light on a unified explain about the different experimental results, and propose the crucial clue to further experiments to elucidate the topological nature of ZrTe_5 and HfTe_5 .

Results

As shown in Fig. 1(a), ZrTe_5 and HfTe_5 share the same base-centered orthorhombic crystal structure with Cmcm (No. 63) space group symmetry. Trigonal prismatic ZrTe_3 chains oriented along the a axis make up the ZrTe_5 natural cleavage plane. Each chain consists of one Zr atom and two different kinds of Te atoms. ZrTe_3 chains are connected by zigzag Te chains along the c axis, building a two dimensional structure of ZrTe_5 in the a - c plane. One crystal unit cell contains two ZrTe_5 planes piled along the b axis, the stacking orientation of ZrTe_5 . The Brillouin zone and its high symmetry k-points of ZrTe_5 (HfTe_5) are shown in Fig. 1(b), in which a^* , b^* , and c^* are the reciprocal lattice vectors.

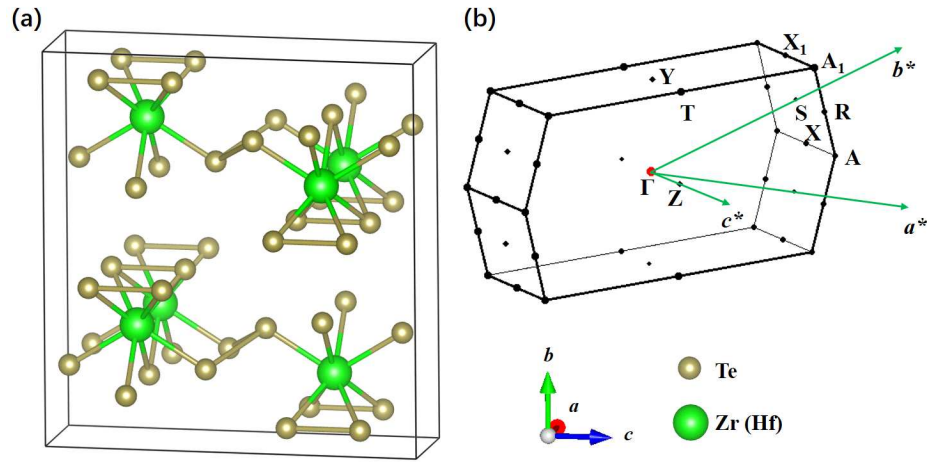


Figure 1. (Color online) (a) Layered crystal structure of ZrTe_5 (HfTe_5) in the orthorhombic conventional unit cell. Big green and small brown balls represent Zr (Hf) and Te atoms respectively. The layers stack along the b direction. (b) Brillouin zone and the high symmetry points of the primitive unit cell of ZrTe_5 (HfTe_5).

Due to the weak the van der Waals (vdw) interaction in the layer ZrTe_5 (HfTe_5),⁹ the vdw corrected correlation functional is necessary in order to obtain the good theoretical lattice constants. In Table I, we present the optimized lattice constants of ZrTe_5 and HfTe_5 based on the optB86b-vdw functional, as well as the experimental ones.²¹ We find that the theoretical and experimental lattice constants are well consistent with each other and the maximum difference between them is less than 1%. For comparison, we also optimized the structures of ZrTe_5 and HfTe_5 by using the standard Perdew-Burke-Ernzerhof (PBE) exchange correlation.²² It is obvious that there is a large error (about 9 %) in the lattice b (in the

Table 1. Calculated and experimental lattice constants and volumes of ZrTe₅ and HfTe₅ in conventional unit cell. Experimental data is from reference 21.

Material	Method	a (Å)	b (Å)	c (Å)	V (Å ³)
ZrTe ₅	PBE	4.0490	15.772	13.845	884.17
	optB86b-vdw	4.0064	14.590	13.732	802.69
	exp. (293 K)	3.9875	14.530	13.724	795.15
	exp. (10 K)	3.9797	14.470	13.676	787.55
HfTe ₅	PBE	4.0245	15.694	13.843	874.37
	optB86b-vdw	3.9799	14.564	13.743	796.58
	exp. (293 K)	3.9713	14.499	13.729	790.51
	exp. (10 K)	3.9640	14.443	13.684	783.44

stacking direction), which indicates that standard PBE failed to describe the structures of ZrTe₅ and HfTe₅, and the vdw correction is necessary.

In order to explore the possible topological phase transition in ZrTe₅ (HfTe₅), we then study their electronic properties under different volumes. Based on the above optimized structure, we change volume of the unit cell by hand and then optimize the atom positions and lattice constants under each variant volumes. This process can simulate the hydrostatic pressure experiments or the thermal expansion effect due to finite temperatures. It is noted that we did not change the volume drastically and the system is far away from the region of superconductivity phase under high pressure found in ZrTe₅ and HfTe₅.^{23–25} In Fig. 2(a), we present the change of lattice constants a , b , and c under different volume expansion ratio, defined as $(V - V_0)/V_0 \times 100\%$, where V_0 is the unit cell volume at theoretical ground state listed in the Table I. It is found that all the lattice constants have similar linear dependence on the volume of the unit cell. But the in-plane lattice constants a and c changes much slower with the volume than that of the lattice constant b , which indicates the weak inter-layer binding energy along the b direction in ZrTe₅. The parabolic-like relationship between total energy of unit cell and volume is expected and given in Fig. 2 (b). The blue vertical dotted line represent the experimental volume at low temperature (10 K), which is nearly 1.9% smaller than our calculated value.

Then we have calculated the band structures and the DOSs with spin-orbit coupling (SOC) under variant volumes, and three of them are shown in Fig. 3. The calculated band structure (Fig. 3 (a)) at the ground state volume ($\Delta V = 0$) is similar as previous theoretical computation⁹, although we use a different high symmetry k-path. A clear direct band gap about 94.6 meV at Γ point is found in the band structure. Of course it is also found that the valence band maxima is between the Γ and Y point and conduction band minima is between the A₁ and T point. Therefore the indirect band gap is much smaller than the direct one at Γ point, which is about 41.7 meV in Fig. 3(a). The present of a clear band gap is confirmed in its corresponding DOS (Fig. 3 (d)). Our calculated band gap is comparable with the values observed in the previous experiments, which is 80 or 100 meV.^{16,17} We also calculated the 3D iso-energy surface (not shown here) of ZrTe₅ in the whole Brillouin zone by the wannier functions and confirmed again that there is a global band gap in ZrTe₅ when $\Delta V = 0\%$.

When ZrTe₅ expands from its ground state, the band gap decreases gradually until the valence and conduction bands touch each other at a critical volume expansion ratio about 2.72%. Then, a Dirac point is formed at Γ point, which can be clearly seen in Fig. 3(b). This behavior is also confirmed in

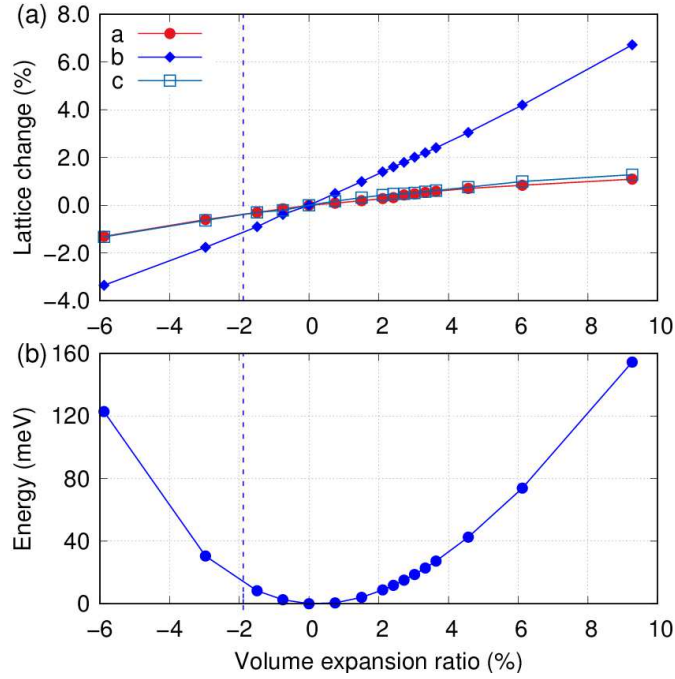


Figure 2. (Color online) (a) Lattice constants a , b , and c under different unit cell volumes. (b) Relative total energy of a primitive unit cell of ZrTe_5 under different volumes. Blue vertical dotted lines represent the experimental volume at 10 K.²¹

its corresponding V-shaped DOS near the Fermi energy, as shown in Fig. 3(e), which is the feature of Dirac point in band structure. It is noted that this Dirac point is 4-fold degenerate since ZrTe_5 has both the space inversion and time reversal symmetry. As the crystal continues to expand, the band gap of ZrTe_5 opens again, and ultimately reaches a value of about 102.6 (direct) or 27.7 meV (indirect) under a volume expansion 6.12%. (see Figure 3 (c) and (f)). This band gap is also confirmed by the 3D iso-energy surface of ZrTe_5 in the Brillouin zone. Therefore from Fig. 3, we can clearly see a transition from a semiconductor to a semi-metal and then to a semiconductor again in ZrTe_5 when it expands. In order to check whether such a transition is topological or not, we have calculated the Z_2 indices under each volume.²⁶ It is found that the Z_2 indices are all (1;110) when the volume expansion is less than 2.72%, while it is (0;110) when the volumes expansion is larger than 2.72%. This definitively confirms that ZrTe_5 undergoes a topological phase transition from a strong TI, to an intermediate Dirac semi-metal state, and finally turns to a weak TI when its unit cell expands from 0 to 6.12% in our calculation. We noted that our calculated weak indices (110) are different from Weng's calculation⁹ but same as Manzoni's¹⁹ since the weak indices of Z_2 depend on the choice of the unit cell.²⁶

The surface states of ZrTe_5 in the strong and weak TI phase have also been calculated based on the wannier functions, shown in Fig. 4. The surface band structures are very similar as the one presented in Weng's work,⁹ since we use the similar high symmetry k-path in the surface Brillouin zone. From Fig. 4, we can see that there is a Dirac point at Γ point in top surface's band structure for the ZrTe_5 of $\Delta V = 0\%$ while it does not for the case of $\Delta V = 6.12\%$. This key difference confirms again that ZrTe_5 is a strong TI when $\Delta V = 0\%$ and it becomes a weak TI when $\Delta V = 6.12\%$.

The detailed phase diagrams of such a topological phase transition of ZrTe_5 and HfTe_5 are given in Fig. 5, in which all the calculated absolute value of direct band gaps at Γ point under different volumes are plotted. In Fig. 5(a) we can find that the band gaps of ZrTe_5 decreases linearly as the volume

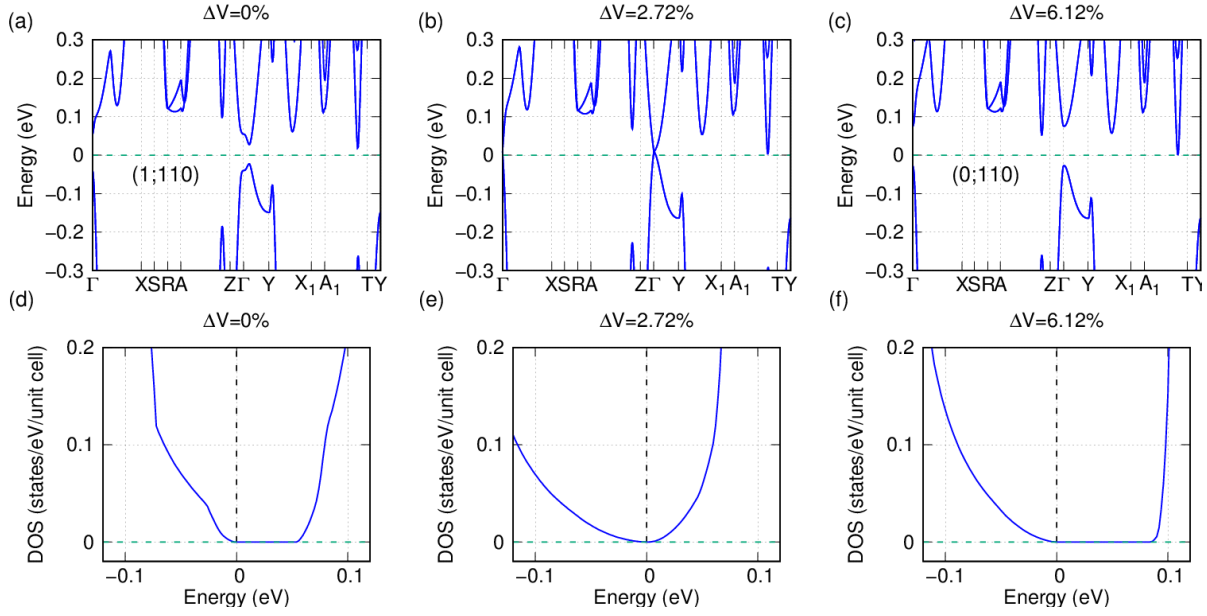


Figure 3. (Color online) Band structures (a-c) and their corresponding DOSs (d-f) with SOC of ZrTe₅ under different volumes. The high-symmetry points are given in Fig. 1(b). Fermi energy is set as 0.

increases from a negative volume expansion ratio about -6%, with a rate around -33 meV per 1% change of volume, where the negative value means a decrease of the band gap when the crystal expands. The band gap disappears at $\Delta V = 2.72\%$. Then it raises linearly with volume in a similar rate of 28 meV per 1% change of volume. Therefore ZrTe₅ undergoes a topological transition from a strong TI to a weak TI due to volume expansion. Such a transition must need a zero-gap intermediate state, which is the Dirac semi-metal state found at about $\Delta V = 2.72\%$ in our calculation. Similar phase diagram is also found recently by Manzoni *et al.*,¹⁹ in which they present the band gap at Γ point as a function of the inter-layer distance, but not the volume of the unit cell. It is known that the mono-layer ZrTe₅ is a quantum spin Hall insulator.⁹ When we stack many mono-layers of ZrTe₅ into a 3D bulk ZrTe₅ crystal, it would be a 3D strong or weak TIs which is depending on the strength of coupling between the adjacent layers. From Manzoni's¹⁹ and our calculation, it is obvious that the inter-layer distance is the key factor that causes the transition between the strong and weak TI phases in ZrTe₅. In Fig. 5(b), we also show that HfTe₅ has the very similar topological phase transition, with almost the same transition critical volume expansion ratio at about 2.72%. The band gap of HfTe₅ also changes linearly as the volume increases with a rate about -31 and 26 meV per 1% change of volume in the strong and weak TI region respectively.

Discussion

The changing rate of our calculated band gap is quite significant especially in a small band gap semiconductor material. Therefore, we can conclude that the electronic properties of ZrTe₅ (HfTe₅) are indeed very sensitive to the change of the volume and they are indeed located very close to the boundary between the strong and weak TI. Although our optimized and the experimentally measured volume of ZrTe₅ (HfTe₅) both indicate that they should be within the strong TI region, we think it still has the possibility that in experiment ZrTe₅ (HfTe₅) can locate in a weak TI region due to different growth methods and characterization techniques in experiments. According to Fig. 5, it is even possible that ZrTe₅ (HfTe₅) can be very close to the intermediate Dirac semi-metal state if it happens that its unit cell has a proper vol-

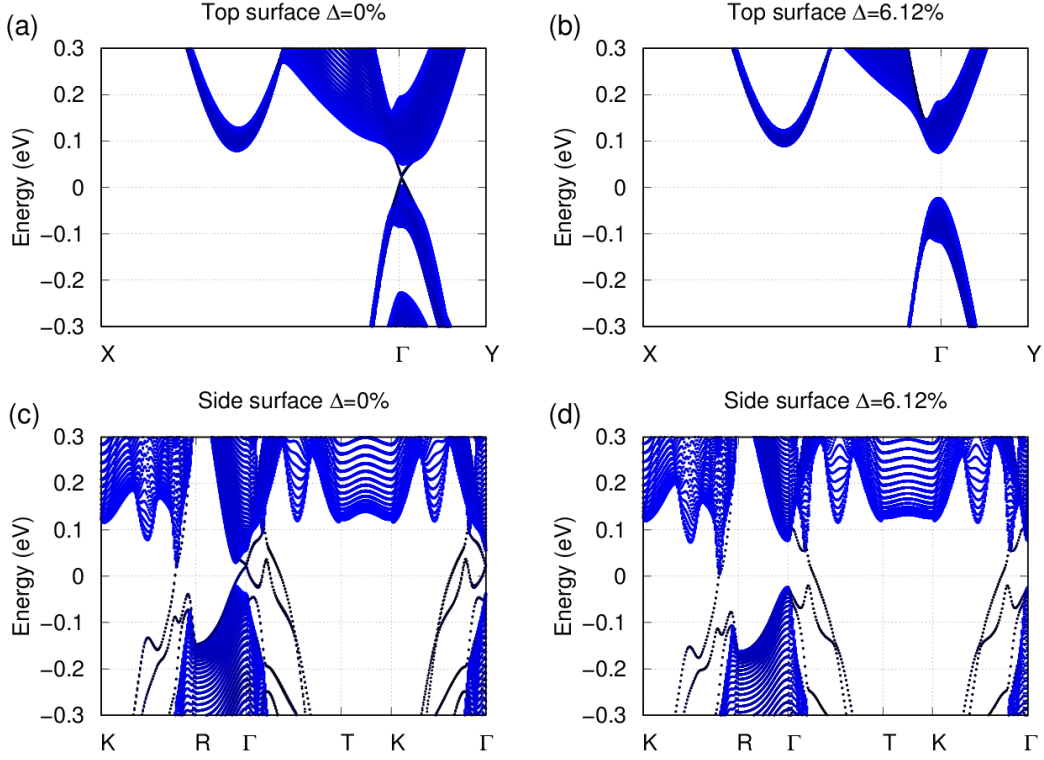


Figure 4. (Color online) Calculated surface states of the top surface (a - c plane, i.e. cleavage surface) for the strong (a) and weak (b) TI phase. Calculated surface states of the side surface (a - b plane) for the strong (c) and weak (d) TI phase. Fermi energy is set as 0.

ume expansion ratio, which, however, is quite challenging in experiment. Another more possible reason which can explain the semi-metal behavior found in experiments is due to the defect and doping, which make the ZrTe_5 (HfTe_5) being a degenerate semiconductor. In a degenerate semiconductor, the Fermi energy is located within the conduction or valence band due to the doping effect, and the crystal will behave like a metal. But in this case, the energy gap still exist just below or above the Fermi energy and the Dirac point is not needed in the energy gap. This possibility is verified in a recent experimental work by Shahi *et al.* They found that the resistance anomaly of ZrTe_5 , which was observed in many current experiments, is due to the Te deficiency, while the nearly stoichiometric ZrTe_5 single crystal shows the normal semiconducting transport behavior.²⁷ In order to avoid the possible artificial effect induced by the cleavage in both STM and ARPES experiments, we suggest that nondestructive optical measurements for the existence of a direct band gap at Γ point, and its change under different temperatures, in the high quality and stoichiometric single crystals are probably useful to elucidate the topological nature in ZrTe_5 and HfTe_5 .

Finally we show the importance of our calculated change rate of band gap. First we can roughly estimate the bulk thermal expansion coefficient from experimental lattice constants of ZrTe_5 (Table I) to be about $3.4 \times 10^{-5} \text{ K}^{-1}$, which means that the volume will change about 1% when the temperature changes from 0 to 300 K, equivalently the band gap of ZrTe_5 at Γ point will change about -33 meV for strong TI phase or 28 meV for weak TI phase, according to our calculation. In a recent high-resolution ARPES work,²⁸ Zhang *et al.* found a clear and dramatic temperature dependent band gap in ZrTe_5 , from which we then can estimate that change rate of observed band gap is about 26 or 37 meV from 0 to 300 K depending on the methods used in their experiment. These two values are both well consistent with our

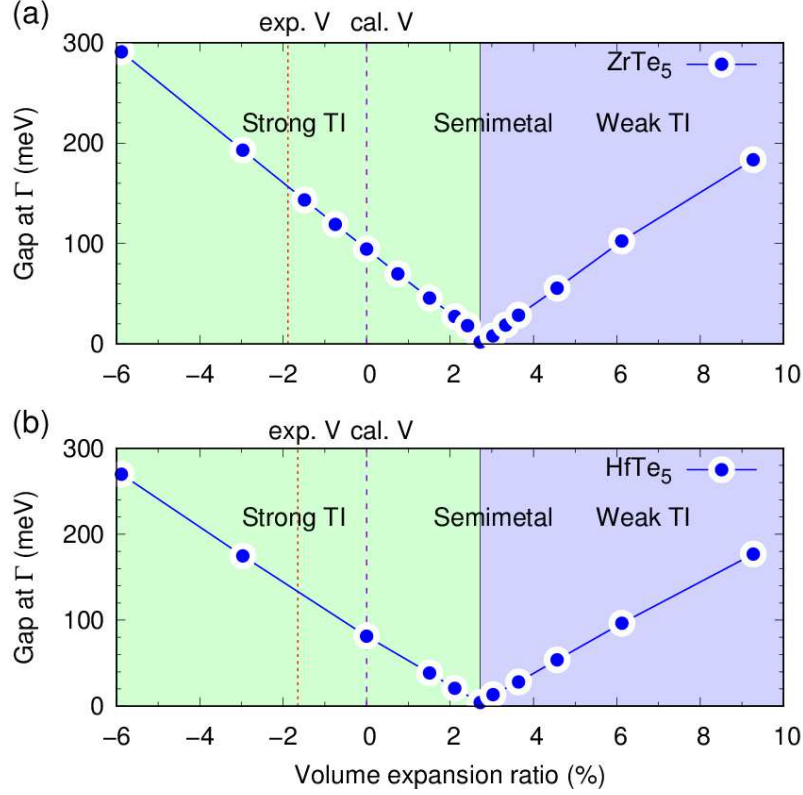


Figure 5. (Color online) (a) Calculated absolute value of direct band gap at Γ point of ZrTe_5 under different volumes. The light green and blue region represent the phases of strong and weak TIs respectively. The boundary between the strong and weak TI is the semi-metal state. The red and blue dotted vertical lines represent the experimental volume at 10 K and calculated one at ground state respectively. (b) Same as (a) but for HfTe_5 .

calculated result. Moreover, the positive change rate found in the experiment ²⁸ implies that the ZrTe_5 crystal used in their experiment is probably a weak TI according to our calculated phase diagram in Fig. 4.

In summary, we have studied the band structures of ZrTe_5 and HfTe_5 at variant volume by first principles calculations. A clearly volume dependent strong and weak topological phase transition is found, accompanied by an intermediate Dirac semi-metal state at the boundary between the transition. The direct band gap of ZrTe_5 at Γ point changes linearly with the volume, which is -33 meV and 28 meV in a strong and weak TI phase respectively, if the volume of ZrTe_5 increases 1%, or equivalently if the temperature increases from 0 to 300 K. The results for HfTe_5 is very similar to those of ZrTe_5 . Our calculated results indicate that the electronic properties and topological nature of ZrTe_5 and HfTe_5 are indeed very sensitive to the lattice constants of crystals, which is probably the reason for the divergent experimental results at present. We suggest that high quality and stoichiometric single crystal with accurate structure refinement at different temperatures would be helpful to resolve the divergent experimental results in ZrTe_5 and HfTe_5 .

Methods

The geometric and electronic properties of ZrTe_5 and HfTe_5 are calculated by the density functional theory in the generalized gradient approximation implemented in the Vienna Ab-initio Simulation Package (VASP) code.^{29,30} The projected augmented wave method^{31,32} and the van der Waals (vdw) corrected optB86b-vdw functional^{33,34} are used. The plane-wave cutoff energy is 300 eV and the k-point mesh is $8 \times 8 \times 4$ in the calculations. And a denser k-point mesh of $24 \times 24 \times 12$ is used in the density of state (DOS) calculation. Spin-orbit coupling (SOC) is included in the calculation except for the structural optimization.

The theoretical ground states of ZrTe_5 and HfTe_5 are obtained by fully optimization of the atom positions and lattice constants, until the maximal residual force is less than 0.01 eV/Å. Then we vary and fix the volumes of unit cell and still optimize the atom positions and lattice constants to study the possible topological transition in ZrTe_5 and HfTe_5 .

The maximally-localized Wannier functions of ZrTe_5 are fitted based on the Zr's d and Te's p orbitals by the Wannier90 code³⁵ and then the surface states are calculated by the WannierTools.³⁶

References

1. Hasan, M. Z. & Kane, C. L. Colloquium: Topological insulators. *Rev. Mod. Phys.* **82**, 3045–3067 (2011).
2. Qi, X. L. & Zhang, S. C. Topological insulators and superconductors. *Rev. Mod. Phys.* **83**, 1057–1110 (2010).
3. Ando, Y. Topological insulator materials. *J. Phys. Soc. Jap.* **82**, 102001–1–32 (2013).
4. Zhang, H. *et al.* Topological insulators in Bi_2Se_3 , Bi_2Te_3 and Sb_2Te_3 with a single Dirac cone on the surface. *Nat. Phys.* **5**, 438–442 (2009).
5. Chen, Y. L. *et al.* Experimental realization of a three-dimensional topological insulator, Bi_2Te_3 . *Science* **325**, 178–181 (2009).
6. Jones, T. E., Fuller, W. W., Wieting, T. J. & Levy, F. Thermoelectric power of HfTe_5 and ZrTe_5 . *Solid State Commun.* **42**, 793–798 (1982).
7. Okada, S., Sambongi, T. & Ido, M. Giant resistivity anomaly in ZrTe_5 . *J. Phys. Soc. Jap.* **49**, 839–840 (1980).
8. DiSalvo, F. J., Fleming, R. M. & Waszczak, J. V. Possible phase transition in the quasi-one-dimensional materials ZrTe_5 or HfTe_5 . *Phys. Rev. B* **24**, 2935–2939 (1981).
9. Weng, H., Dai, X. & Fang, Z. Transition-metal pentatelluride ZrTe_5 and HfTe_5 : A paradigm for large-gap quantum spin Hall insulators. *Phys. Rev. X* **4**, 011002 (2014).
10. Chen, R. Y. *et al.* Magnetoinfrared spectroscopy of Landau levels and Zeeman splitting of three-dimensional massless Dirac fermions in ZrTe_5 . *Phys. Rev. Lett.* **115**, 176404 (2015).
11. Chen, R. Y. *et al.* Optical spectroscopy study of the three-dimensional Dirac semimetal ZrTe_5 . *Phys. Rev. B* **92**, 075107 (2015).
12. Li, Q. *et al.* Chiral magnetic effect in ZrTe_5 . *Nat. Phys.* **12**, 550–555 (2016).
13. Liu, Y. W. *et al.* Zeeman splitting and dynamical mass generation in Dirac semimetal ZrTe_5 . *Nat. Commun.* **7**, 12516 (2016).

14. Yuan, X. *et al.* Observation of quasi-two-dimensional Dirac fermions in ZrTe₅. *arXiv* 1510.00907 (2015).
15. Zheng, G. *et al.* Transport evidence for the three-dimensional Dirac semimetal phase in ZrTe₅. *Phys. Rev. B* **93**, 115414 (2016).
16. Li, X. B. *et al.* Experimental Observation of Topological Edge States at the Surface Step Edge of the Topological Insulator ZrTe₅. *Phys. Rev. Lett.* **116**, 176803 (2016).
17. Wu, R. *et al.* Evidence for Topological Edge States in a Large Energy Gap near the Step Edges on the Surface of ZrTe₅. *Phys. Rev. X* **6**, 021017 (2016).
18. Moreschini, L. *et al.* Nature and topology of the low-energy states in ZrTe₅. *Phys. Rev. B* **94**, 081101 (2016).
19. Manzoni, G. *et al.* Evidence for a Strong Topological Insulator Phase in ZrTe₅. *Phys. Rev. Lett.* **117**, 237601 (2016).
20. Manzoni, G. *et al.* Temperature dependent non-monotonic bands shift in ZrTe₅. *J. Electron Spectrosc. Relat. Phenom.* in press (2016).
21. Fjellvag, H. & Kjekshus, A. Structural properties of ZrTe₅ and HfTe₅ as seen by powder diffraction. *Solid State Commun.* **60**, 91–93 (1986).
22. Perdew, J. P., Burke, K. & Ernzerhof, M. Generalized gradient approximation made simple. *Phys. Rev. Lett.* **77**, 3865–3868 (1996).
23. Zhou, Y. *et al.* Pressure-induced superconductivity in a three-dimensional topological material ZrTe₅. *PNAS* **113**, 2904–2909 (2016).
24. Qi, Y. *et al.* Pressure-driven Superconductivity in Transition-metal Pentatelluride HfTe₅. *Phys. Rev. B* **94**, 054517 (2016).
25. Liu, Y. *et al.* Superconductivity in HfTe₅ Induced via Pressures. *arXiv* 1603.00514 (2016).
26. Soluyanov, A. A. & Vanderbilt, D. Computing topological invariants without inversion symmetry. *Phys. Rev. B* **83**, 235401 (2011).
27. Shahi, P. *et al.* Bipolar Conduction is the Origin of the Electronic Transition in Pentatellurides: Metallic vs. Semiconducting Behavior. *arXiv* 1611.06370 (2016).
28. Zhang, Y. *et al.* Electronic Evidence of Temperature-Induced Lifshitz Transition and Topological Nature in ZrTe₅. *arXiv* 1602.03576 (2016).
29. Kresse, G. & Hafner, J. Ab initio molecular dynamics for open-shell transition metals. *Phys. Rev. B* **48**, 13115–13118 (1993).
30. Kresse, G. & Furthmüller, J. Efficiency of ab-initio total energy calculations for metals and semiconductors using a plane-wave basis set. *Comput. Mater. Sci.* **6**, 15–50 (1996).
31. Blöchl, P. Projector augmented-wave method. *Phys. Rev. B* **50**, 17953–17979 (1994).
32. Kresse, G. & Joubert, D. From ultrasoft pseudopotentials to the projector augmented-wave method. *Phys. Rev. B* **59**, 1758–1775 (1999).
33. Klimes, J., Bowler, D. R. & Michaelides, A. Chemical accuracy for the van der Waals density functional. *J. Phys.: Condens. Matter* **22**, 022201 (2009).

34. Klimes, J., Bowler, D. R. & Michaelides, A. Van der Waals density functionals applied to solids. *Phys. Rev. B* **83**, 195131 (2011).
35. Mostofi, A. A. *et al.* An updated version of wannier90: A tool for obtaining maximally-localised Wannier functions. *Comput. Phys. Commun.* **185**, 2309 (2014).
36. Wu, Q. S. & Zhang, S. N. WannierTools: An open-source software package for novel topological materials URL https://github.com/quanshengwu/wannier_tools.

Acknowledgements

This work is supported by the National Key R&D Program of China (2016YFA0201104), the State Key Program for Basic Research (No. 2015CB659400), and the National Science Foundation of China (Nos. 91622122, 11474150 and 11574215). The use of the computational resources in the High Performance Computing Center of Nanjing University for this work is also acknowledged.

Author contributions statement

Y.B.C., S.H.Y., and J.Z. proposed the idea. Z.J.F., Q.F.L. and J.Z. carried out the calculations, analysed the results, and plotted the figures. Z.J.F. and J.Z. wrote the manuscript. All authors reviewed the manuscript.

Additional information

Competing financial interests: The authors declare no competing financial interests.